Effect of Soil-Structure Interaction on Seismic Risk of FAN Type Cable Stayed Bridges

R.A. Khan[1], S. Ahmad[2] and T.K. Datta[3]

1. Civil Engineering Department, Jamia Millia Islamia, New Delhi-25, India, email: rehan_iitd@rediffmail.com
2. Applied Mechanics Department, Indian Institute of Technology, New Delhi-16, India
3. Civil Engineering Department, Indian Institute of Technology, New Delhi-16, India

ABSTRACT: *Probabilistic Risk Analysis (PRA) of fan type cable stayed bridges is presented to determine their probabilities of failure under random ground motion. Seismic input to the bridge support is considered to be a risk consistent response spectrum. The bridge deck is modeled as a beam supported on springs at different points. The coupled stiffness matrix of the springs is determined by a separate 2D static analysis of cable-tower-deck system in which flexibility of the tower base due to soil-structure interaction is included. Damping due to soil is incorporated by the equivalent modal energy method. The response of the bridge deck is obtained by the response spectrum method of analysis for multi-degree of freedom system. The PRA includes uncertainties of responses due to the variation in ground motion, material property, modeling and method of analysis, and uncertainties of the capacity due to the variation of ductility factor and damage concentration effect. Failure mode of the bridge is assumed to be bending failure of the bridge deck at the point of maximum bending moment. Probability of failure of the bridge deck is determined by First Order Second Moment theory of reliability analysis. A three span double plane symmetrical fan type cable stayed bridge is used as an illustrative example. The fragility curves for the bridge deck failure are obtained under a number of parametric variations. The parameters include, base flexibility, degree of correlation of ground motion, angle of incidence of earthquake, ratio of the components of ground motion, and seismic input. The study shows that flexible base condition provides significantly less value of probability of failure as compared to the fixed base. Further, angles of incidence, degree of correlation, ratio of components of ground motion and input response spectrums have considerable effects on the probability of failure.*

Keywords: Bridges; Structural response; Soil–Structure Interaction; Reliability analysis

1. Introduction

Recently, several cable stayed bridges have been constructed on relatively soft ground, which results in a great demand to evaluate the effect of soil-structure interaction (*SSI*) on the seismic behaviour of such bridges, and properly reflect it in seismic design. A number of studies have been conducted in recent years to comprehend the effects of *SSI* on the seismic behaviour of bridges [1, 2, 3], which have shown that *SSI* generally tends to elongate the natural periods of bridge-foundation-soil systems, and may significantly affect internal forces in structural members and displacement response of bridges. It has also been recognized that the way in which *SSI* affects the seismic behaviour of bridges depends on the conditions of the bridge-foundation-soil system [4], suggesting a necessity to perform many detailed

case studies.

Although the studies such as above, have demonstrated the significance of *SSI*, and provided many constructive results, very few studies have focused on the effect of *SSI* on the reliability estimates of long span cable supported bridges to environmental loading. Long span bridge, being flexible in nature, becomes more flexible due to *SSI*. As a result, they may be more affected by low frequency wind excitation and the reliability of the bridges against long term (fatigue) or short term (first passage) failure is expected to be lowered by the *SSI* effect. As far as the seismic forces are concerned, the effect of *SSI* on the reliability estimate needs elaborate study since it not only depends upon the elongated period of the structure, but also on the frequency contents of the seismic forces. Both elongation of the structural period and the frequency contents of the earthquake depend upon the soil conditions and therefore, effect of SSI in case of the seismic excitation becomes more complex.

In the present paper, a reliability estimate of fan type cable stayed bridges for earthquake forces is obtained by considering the soil-structure interaction. A simplified equivalent modal energy method [5] in which the soil is replaced by spring-dashpot system is used for including *SSI* effect. The damping coefficients and spring stiffness coefficients are obtained from the results of the half space analysis of rigid circular footing as given by Veletsos and Wei [6]. This has been done only for illustrative purpose and for the ease of calculation. The *PRA* is performed for obtaining the seismic reliability of cable stayed bridge located in a region which is surrounded by three earthquake sources. For the response analysis, a risk consistent response spectrum obtained from a separate analysis is used as seismic input. For the *PRA*, the uncertainties included in the structure are those due to uncertainties of seismic inputs, material property, capacity of the bridge cross section, modeling, analysis procedure, ductility effect and damage concentration effect. The probability of failure is obtained by *FOSM* method of reliability analysis. Effects of a number of important parameters such as the ratio of the components of ground motion, spatial correlation of ground motion, angle of incidence of earthquake, base flexibility etc. on the probability of failure are investigated for a double plane symmetric fan type cable stayed bridge.

2. Assumptions

The following assumptions are made for the study:

i) The bridge deck (girder) and the towers are assumed to be axially rigid.

ii) The bridge deck, assumed as continuous beam, does not transmit any moment to the towers through the girder-tower connection.

iii) Cables are assumed to be straight under high initial tension due to the dead load and well suited to support negative force increment during vibration without losing its straight configuration.

iv) Beam-column effect, in the stiffness formulation of the beam, is considered for the constant axial force in the beam due to dead load effect; fluctuating component due to bridge vibration is ignored.

v) Little earthquake data is available for the region under study, except for the recurrence interval of earthquakes and some indirectly evaluated magnitudes of earthquakes.

vi) The region is surrounded by multiple sources (point sources) of earthquake.

vii) Any of the attenuation laws (reported in the literature) could be valid for the region.

viii) It is assumed that both normalized response spectrum ordinates normalized with respect to maximum acceleration value ($S_N(T)$) is empirically determined function of magnitude M and epicentral distance R, and they are log-normally distributed.

3. Estimation of Equivalent Modal Damping of Soil

The equations of motion of cable stayed bridge shown in Figure (1) can be written in the usual form as

$$[M]\{\ddot{X}\}+[C]\{\dot{X}\}+[K]\{X\}=\{P(t)\} \qquad (1)$$

in which $[M]$ is the diagonal lumped mass-matrix; $[K]$ is the stiffness-matrix corresponding to the dynamic degree of freedom as shown in Figure (1); $[C]$ is the damping-matrix not explicitly known but will be defined in terms of an equivalent modal damping; $\{X\}$ is the displacement vector which includes the base degree of freedom as well; $\{P(t)\}$ is the vector of excitation; dot denotes time derivative.

For the soil, only velocity proportional damping is considered because it reasonably represents the radiation (geometric) damping in elastic half-space and internal (hysteretic) damping of the soil is neglected. The soil damping and stiffness corresponding to the base degrees of freedom are considered frequency independent (i.e. the values of impedance function at zero frequencies) and are

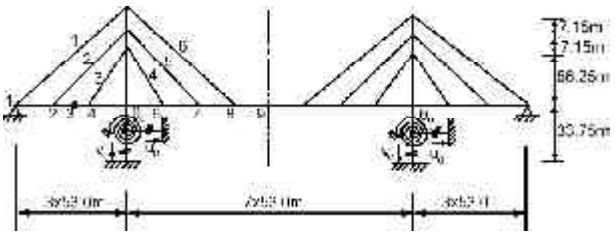

Figure 1. Simplified model for the soil-structure interaction.

taken as those given by Veletsos and Wei [6].

$$K_x = 8Gr_0/(2-\mu) \tag{2a}$$

$$K_{?} = 8Gr_0^3/3(1-\mu) \tag{2b}$$

$$K_{x?} = K_{?x} = 0.6GR^2/(2-\mu) \tag{2c}$$

$$K_v = 4Gr_0/(1-\mu) \tag{2d}$$

$$C_x = 4.8Gr_0/(2-\mu) \tag{2e}$$

$$C_\theta = 0.4Gr_0^3/3(1-\mu) \tag{2f}$$

$$C_{x\theta} = C_{\theta x} = 0.4Gr_0^2/(2-\mu) \tag{2g}$$

$$C_v = 3.04Gr_0/(1-\mu) \tag{2h}$$

in which K_x, K_v, K_θ and $K_{x\theta} = K_{\theta x}$ are the horizontal, vertical , rotational and coupled stiffness coefficients respectively. Similarly, C_x, C_v , C_θ and $C_{\theta x} = C_{x\theta}$ are the dashpot constants. G, r_0 and μ are the modulus of rigidity, radius of the circular foundation and poisson's ratio respectively.

Omitting the damping and excitation terms in Eq.(1), undamped natural frequencies ω_i and the orthogonal mode-shapes $\{\phi_i\}$ can be determined by solving the following eigenvalue problem

$$[M]\{\ddot{X}\} + [K]\{X\} = \{0\} \tag{3}$$

With the individual modes $\{\phi_i\}$ listed as columns, the complete mode-shape matrix $[\phi]$ can be used to describe the response $\{X\}$ in terms of generalized (or normal) coordinates q, as

$$\{X\} = [\phi]\{q(t)\} \tag{4}$$

Substituting Eq. (4) in Eq. (3) and premultiplying by the transpose of the mode-shape matrix i.e. $[\phi]^T$ the equations in generalized coordinates are obtained as:

$$[\overline{M}]\{\ddot{q}\} + [\phi]^T[C][\phi]\{\dot{q}\} + [\overline{K}]\{q\} = [\phi]^T\{P\} \tag{5}$$

in which $[\overline{M}]$ and $[\overline{K}]$ are diagonal matrices of generalized mass and stiffness.

With the damping of soil included, the damping-matrix $[\phi]^T[C][\phi]$ always has off-diagonal terms because of which Eq. (5) cannot be split up into independent single degree of freedom (*SDOF*) equations in generalized coordinates. However, an equivalent total damping in each mode of vibration of the flexible-base structure can be obtained in the following way [5].

Assume that each mass of the bridge is free to undergo horizontal translation u, vertical translation v and rotation θ and that the bridge and footing are harmonically vibrating in the i-th mode with natural frequency ω_i. The natural frequencies and modes can approximately be considered equal to those of an undamped system [as given by Eq. (3)]. The footing has the following displacements corresponding to the three base degrees of freedom (Figure (1)) u_0, v_0 and θ_0.

In general, the work done W_d by the damping forces $F(x)$, during a period of vibration $T = 2\pi/\omega_i$ is given by

$$W_d = \int_0^T F(x)\,dx(t) \tag{6}$$

This formula can be used to find the work done by the footing's equivalent damping (dashpots) during the vibration of the bridge in a natural mode. During harmonic motions expressed as

$$u_0(t) = u_0 \sin\omega_i t \tag{7a}$$

$$v_0(t) = v_0 \sin\omega_i t \tag{7b}$$

$$\theta_0(t) = \theta_0 \sin\omega_i t \tag{7c}$$

The resistive forces due to damping corresponding to the base degrees of freedom are

$$P = P(\dot{u}_0) + P(\dot{?}_0) + P(\dot{v}_0) \tag{8a}$$

$$M = M(\dot{?}_0) + M(\dot{u}_0) + M(\dot{v}_0) \tag{8b}$$

in which the damping forces acting at the footing are

$$P(\dot{u}_0) = c_x\dot{u}_0(t) = c_x u_0\omega_i\cos\omega_i t \tag{8c}$$

$$P(\dot{v}_0) = c_v\dot{v}_0(t) = c_v v_0\omega_i\cos\omega_i t \tag{8d}$$

$$P(\dot{\theta}_0) = c_{x\theta}\dot{\theta}_0(t) = c_{x\theta}\theta_0\omega_i\cos\omega_i t \tag{8e}$$

$$M(\dot{u}_0) = c_{\theta x}\dot{u}_0(t) = c_{\theta x}u_0\omega_i\cos\omega_i t \tag{8f}$$

$$M(\dot{\theta}_0) = c_\theta\dot{\theta}(t) = c_\theta\theta_0\omega_i\cos\omega_i t \tag{8g}$$

$$M(\dot{v}_0) = c_v v_0\omega_i\cos\omega_i t \tag{8h}$$

According to Eq. (6), the total work done by these forces during a period of vibration T in the i-th mode is

$$W_{di} = \int_0^T c_x u_0^2 \omega_i^2 cos^2 ?_i t.dt + \int_0^T c_? ?_0^2 \omega_i^2 cos^2 \omega_i t.dt + \int_0^T c_v v_0^2 \omega_i^2 cos^2 \omega_i t.dt + 2\int_0^T c_{?x} ?_0 u_0 \omega_i^2 cos^2 \omega_i t.dt \quad (9)$$

which simplifies to

$$W_{di} = \pi \omega_i (c_x u_0^2 + 2c_{?x} u_0 ?_0 + c_? ?^2 + c_v v_0^2) \quad (10)$$

The maximum potential energy of the bridge in the i-th mode can be calculated as max. kinetic energy ϕ_{pi} given by

$$\phi_{pi} = \sum_{j=0}^{n} 1/2 m_j u_j^2 \omega_i^2 + \sum_{j=0}^{n} (1/2 I_j ?_j^2 ?_i^2 + 1/2 m_j v_j^2 \omega_i^2) \quad (11)$$

where n is the number of masses; m_j is the j-th mass; and I_j is the j-th mass moment of inertia.

The damping ratio η_g of the structure due to the geometric damping of the soil is defined for the response in the i-th mode as

$$?_{gi} = W_{di} / 4p\phi_{pi} \quad (12)$$

Substituting for W_{di} and ϕ_{pi} from Eqs. (10) and (11) in Eq. (12), the following expression for η_{gi} is obtained as

$$n_{gi} = (1/2\overline{m} ?_i)(c_x u_0^2 + c_v v_0^2 + 2c_{\theta x} u_0 \theta_0 + c_\theta ?_0^2) \quad (13)$$

in which $\overline{m}_i$ is the generalized mass given by

$$\overline{m}_i = \phi^T M \phi \quad (14)$$

In the above equations, ϕ and M are the mode shapes coefficient and mass matrix of the bridge while u_0, v_0 and θ_0 are the modal displacements of the footing obtained from the solution of Eq. (3); c_x, c_v and c_θ are the soil damping constants which are given by Eqs.(2a) to (2h) considered in the analysis.

The damping due to the soil η_{gi} (determined above) can be added to the other component of damping i.e., the modal damping η_i of the bridge to get the total damping η_i^t for the i-th mode.

$$\eta_i^t = \eta_i + \eta_{gi} \quad (15)$$

4. Risk Consistent Response Spectrum and Coherence Function

For obtaining the risk consistent response spectrum at the free field, a risk consistent response spectrum at the bedrock level is first derived using a procedure outlined by Shinozuka, M. et al [7]. The procedure assumes that the occurrence of earthquake is a poisson process and considers the effect of several earthquake sources which surround a given region. The methodology requires the construction of a conditional probability matrix of the form $P(A \geq a | M_i)_k$ in which A denotes PGA; a is specified value of the PGA; M_i is the i^{th} value of the magnitudes of earthquake for which the conditional probability of the exceedance of PGA is obtained; k is the k^{th} source of earthquake surrounding the region. Since it is assumed that not much earthquake data is available, it is very difficult to construct the conditional probability for the region given by $[P(A \geq a) | M_i]_k$ in which A denotes PGA; a is specified value of the PGA; M_i is the i^{th} value of the magnitudes of earthquake for which the conditional probability of the exceedance of PGA is obtained; k is the k^{th} source of earthquake surrounding the region. Therefore, help of available attenuation laws is taken to construct this conditional probability. Since it is also not possible to verify the applicability of any attenuation law for the region, it is assumed that any attenuation law out of a collected set of attenuation laws could be valid for the region. Thus, for a given magnitude of earthquake, the PGA value at any epicentral distance defining the site, becomes a random variable. The set of values (say N values), the random variable can assume, is obtained from the set of attenuation laws considered in the study. For example, if N is the number of attenuation laws selected, then N values of PGA are obtained for a given magnitude of earthquake at the site. The probability of occurrence of a PGA value at the site can be then obtained from the N values of the PGA for a given magnitude of earthquake. An empirical relationship is used to obtain the logarithmic spectral acceleration ordinates for different period as function of magnitude of earthquake and epicentral distance [8]. Response spectrum at the free field is obtained by one dimensional wave propagation analysis through the soil with the input spectrum at the bedrock. The free field risk consistent response spectrum is used as input to the bridge. Apart from the response spectrum, the response analysis of multi-supported structures like bridge requires the specification of a coherence function. This function takes into consideration the lack of correlation between ground motions at different supports in the seismic analysis of the bridge. In the present analysis, the coherence function used is given in the next section (Eq. (21)).

5. Response Analysis of Cable Stayed Bridge

Using modal spectral analysis, the variance of the total vertical displacement of the bridge deck can be obtained by integrating the psdf of the total vertical

displacement over the frequency range of interest and is given by

$$\sigma_Y^2(x_r) = \sum_{j=1}^{8}\sum_{k=1}^{8}\sum_{n=1}^{M}\sum_{m=1}^{M}\phi_n(x_r)\phi_m(x_r)\gamma_{jn}\gamma_{km}\rho_{f_{jn}f_{km}}\sigma_{f_{jn}}\sigma_{f_{km}} + 2\sum_{j=1}^{8}\sum_{k=1}^{8}\sum_{n=1}^{M}\phi_n(x_r)\gamma_{jn}g_{kr}(x_r)\rho_{f_{jn}f_k}\sigma_{f_{jn}}\sigma_{f_k} + \sum_{j=1}^{8}\sum_{k=1}^{8}g_{jr}(x_r)g_{kr}(x_r)\rho_{f_j f_k}\sigma_{f_j}\sigma_{f_k} \quad (16)$$

in which

$$\sigma^2_{f_{jn}} = \int_{-\alpha}^{\alpha}|H_n(\omega)|^2 S_{\ddot{f}_j\ddot{f}_j}(\omega)\,d\omega$$
$$\sigma^2_{f_j} = \int_{-\alpha}^{\alpha} S_{f_j f_j}(\omega)\,d\omega \quad (17)$$

$$\rho_{f_{jn}f_{km}} = \frac{1}{\sigma_{f_{jn}}\sigma_{f_{km}}}\int_{-\alpha}^{\alpha}H^*_n(\omega)H_m(\omega)S_{\ddot{f}_j\ddot{f}_k}(\omega)d\omega \quad (18)$$

$$\rho_{f_{jn}f_k} = \frac{1}{\sigma_{f_{jn}}\sigma_{f_k}}\int_{-\alpha}^{\alpha}H^*_n(\omega)S_{\ddot{f}_j f_k}(\omega)d\omega \quad (19)$$

$$\rho_{f_j f_k} = \frac{1}{\sigma_{f_j}\sigma_{f_k}}\int_{-\alpha}^{\alpha}S_{f_j f_k}(\omega)d\omega \quad (20)$$

in which g_{kr} is quasi-static vertical displacement of r^{th} beam segment due to unit displacement; $\phi_n(x_r)$ is n^{th} mode shape of the r^{th} beam segment of the bridge deck; γ_{jn} is modal participation factor; $H_n(\omega)$ is n^{th} modal frequency response function; $S_{\ddot{f}_j\ddot{f}_k}, S_{\ddot{f}_j f_k}, S_{f_j f_k}$ are cross psdfs between support excitation; $\rho_{f_{jn}f_{km}}$ is the cross correlation between mode shapes; $\rho_{f_{jn}f_k}$ is cross correlation between mode shapes and support and $\rho_{f_j f_k}$ is cross correlation between supports.

In obtaining, the cross spectrums $S_{f_j f_k}(\omega)$ etc., the coherence function $\rho_{ij}(\omega)$ is given by

$$\rho_{ij}(\omega) = exp\left[-c\left(\frac{r_{ij}\omega}{2\pi V_s}\right)\right] \quad (21)$$

where r_{ij} is the separation between two stations i and j; V_s is shear wave velocity; ω is frequency of ground motion and c is constant depending on the epicentral distance and inhomogeinity of the medium.

The development of the response spectrum method of analysis which gives the variance of response as given by Eq.(16), is briefly presented below.

Let $D_j(\omega_n, \xi_n)$ denote the response spectrum for the displacement corresponding to the j^{th} support degree of freedom for the frequency ω_n and damping ξ_n and let $f_{j,\,max}$ be the mean peak ground displacement corresponding to the j^{th} support degree of freedom defined as

$$D_j(\omega_n, \xi_n) = p_{jn}\sigma_{f_{jn}} \quad ; \quad f_{j,max} = p_j\sigma_{f_j} \quad (22)$$

The relationship between the expected peak and $r.m.s$ values of response can be written as $f_{j,max} = E[max|f_j(t)|]$ in which p_{jn} and p_j are the peak factors. Similarly, $E[max|Y(x_r,t)|]$ can be written as $E[max|f_{j(t)}|] = p_r\sigma_{f_j}$ in which p_r is the peak factor of the total response. Using Eqs. (17), (18), (19), (20) and assuming that all peak factors p_{jn}, p_j and p_r are the same, the expected peak value of the total displacement can be written as

$$E[max|Y(x_r,t)|] = \Big[\sum_{j=1}^{8}\sum_{k=1}^{8}\sum_{n=1}^{M}\sum_{m=1}^{M}\phi_n(x_r)\phi_m(x_r)\gamma_{jn}\gamma_{km}\rho_{f_{jn}f_{km}} \times D_j(\omega_n,\xi_n)D_k(\omega_m,\xi_m) + 2\sum_{j=1}^{8}\sum_{k=1}^{8}\sum_{n=1}^{M}\phi_n(x_r)\gamma_{jn}g_{kr}(x_r)\rho_{f_{jn}f_k}D_j(\omega_n,\xi_n)f_{k,max} + \sum_{j=1}^{8}\sum_{k=1}^{8}g_{jr}(x_r)g_{kr}(x_r)\rho_{f_j f_k}f_{j,max}f_{k,max}\Big]^{\frac{1}{2}} \quad (23)$$

Similar expression can be obtained for the expected peak value of total vertical bending moment at any point of the bridge deck by replacing $\phi(x_r)$ and $g_{jr}(x_r)$ by $E_d I_r d^2\phi/dx^2$ and $E_d I_r d^2 g_{jr}(x_r)/dx^2$ respectively. The expected peak value of the total response as given by Eq. (23) can be obtained using the response spectrum as input provided $\rho_{f_{jn}f_{km}}, \rho_{f_{jn}f_k}, \rho_{f_j f_k}$ are known. These quantities are obtained by converting the response spectrum to power spectral density function using the expression given by Kiureghian [9] and the coherence function. Thus, the expected peak value of the response is obtained with inputs as the risk consistent response spectrum and a coherence function.

6. Evaluation of Probability of Failure

The load action i.e. moment at any section of the bridge is a random variable due to a number of uncertainties associated with earthquake loading, material properties, method of analysis etc. Similarly, the moment capacity of the section is also a random variable influenced by

many uncertainties like uncertainty of material strength, ductility at the joints, damage concentration effect, etc.

The moment induced at a section (called Resistance *R*), a random variable, is considered to be a product of five random variables and is given by

$$R = M\, F_1\, F_2\, F_3\, F_4 \tag{24}$$

where *M* is a random variable denoting the internal moment at the section produced by the earthquake load. Apart from the random nature of the earthquake loading, the randomness of the moment *M* arises from a number of uncertainties. Out of those four uncertainties are included in the study namely, (i) uncertainty of input motion and soil properties; (ii) uncertainty in system parameter; (iii) uncertainty in modeling; and (iv) uncertainty in the analysis procedure such as non-linear analysis being replaced by linear analysis; mean peak response being obtained from response spectrum analysis rather than Monte Carlo simulation technique and performing a simplified *SSI* analysis. These uncertainties are incorporated in the form of Eq. (24) with the help of four independent random variables F_1 to F_4 representing deviation of the actual response from *M*. The random variables *M*, F_1, F_2, F_3 and F_4 are assumed to be log-normally distributed. As a result,

$$\sigma_{lnR} = \sqrt{\beta_1{}^2 + \beta^2{}_2 + \beta_3{}^2 + \beta_4{}^2} \tag{25}$$

in which β_i, i = 1 to 4 is the coefficient of variation of random variables F_i, i = 1 to 4 and σ_{lnR} is the logarithmic standard deviation of resistance *R*.

Note that the median values of F_1, F_2, F_3 and F_4 are taken as unity and $\sigma^2_{ln\,x} = ln(\beta^2{}_x + 1)$ for $\beta_x \le 0.25$, $\sigma_{ln_x} = \beta_x$ in which β_x is the coefficient of variation of *x*.

Similarly, capacity of the section is written as

$$C = Mc\, F_5\, F_6 \tag{26}$$

where *Mc* is a random variable denoting the moment capacity and F_5 and F_6 are two random variables representing deviation from the actual strength accommodating capacity to resist induced moment at the section. F_5 is incorporated to account for uncertainties due to energy absorption capacity and ductility effect. F_6 caters to the uncertainty due to damage concentration effect in *MDOF* system i.e., actual difference between linear and non-linear analysis of *MDOF* system. All the three random variables are assumed to be independent log-normally distributed variables. Therefore, logarithmic standard deviation of *C* can be written as

$$\sigma_{lnC} = \sqrt{(\beta_5{}^2 + \beta_6{}^2 + \beta_{Mc}{}^2)} \tag{27}$$

in which β_5, β_6 and β_{Mc} are coefficients of variation of F_5, F_6 and *Mc* respectively. The median values of F_5, F_6 and *Mc* are specified.

First Order Second Moment (*FOSM*) method is used to calculate the probability of failure by assuming both resistance *R* and capacity *C* to be log-normally distributed and by defining the probability of failure as given by the standard expression

$$P_f = F\left[\frac{(ln(\overline{R}/\overline{C}))}{(\sigma^2_{lnR} + \sigma^2_{lnC})^{\frac{1}{2}}}\right] \tag{28}$$

where, $\overline{R}$ and $\overline{C}$ are the median values and σ_{lnR} and σ_{lnC} are the logarithmic standard deviation of the resistance and capacity of the structure.

7. Evaluation of Factors (F_1 to F_6)

F_1 represents the variability of response caused by input motion's variability. The median value is unity and the logarithmic standard deviation β_1 is evaluated from two response values corresponding to input motions of the median and 84% non-exceedence spectra i.e $\beta_1 = 1n(r_{84}/r_{50})$. F_2 is the factor representing the variability resulting from the system parameter variation. The logarithmic standard deviation β_2 is evaluated in the same manner as β_1 i.e , as the logarithm of the ratio between the 84^{th} percentile non-exceedence and the median responses. F_3 accounts for the uncertainty involved in the modeling of the system and in the analytical methods for the evaluation of response. It follows that F_3 is to be evaluated as the ratio of observed response to the response calculated with the model. Generally, the median value of F_3 is taken as unity and coefficient of variation ranges between 0. 15 to 0.2 [10]. F_4 is the factor accounting for the uncertainty resulting from the simplifications in the analysis and in the evaluation of the expected response. F_4 is assumed to have a median value of unity with a coefficient of variation as 0.15 [10]. Additionally, uncertainty in the soil properties is incorporated by factor F_2 while uncertainty due to approximations in the SSI analysis is incorporated in factor F_4. The concept of F_5, the energy absorption factor, cater to the energy absorption during nonlinear excursion of a *SDOF* system. The median value is generally taken to be proportional to the Newmark's formula $\sqrt{(2\mu - 1)}$ with reduction factor of 0.6, where μ is the ductility factor. F_6 caters to the damage concentration effect of *MDOF* systems. The median

value of F_6 is evaluated as an average ratio between the linear and nonlinear analysis (for a number of cases on *MDOF* systems). Extensive studies indicate that the median value typically lies in between 0.6 to 1.25. The coefficient of variation is assumed to be 0.1 [10]. Although the above values have been adopted for the factors F_1 to F_6 for obtaining the probabilities of failure (P_f) for the parametric studies, a separate sensitivity analysis has been conducted to investigate the effect of these factors on the P_f..

8. Determination of the Probability of Failure

Once the modal frequencies and the equivalent modal damping η_i^t are known, the equivalent lateral load for each modal vibration can be obtained from the response spectrum as described in previous section. The probability of failure of the bridge with springs is then obtained using the simplified *PRA* procedure as mentioned in the previous sections.

9. Numerical Study

In order to illustrate the *PRA* procedure adopted for finding the reliability of cable stayed bridge with flexible support under seismic excitation, a fan type cable stayed bridge taken by Au et al [11] is considered as shown in Figure (1). The bridge is assumed to be located in a site surrounded by three earthquake sources. The attenuation laws used for obtaining the risk consistent spectrum are taken from [12]. The empirical formula for spectral ordinates is taken from [8]. The other data for obtaining the spectrum use (i) epicentral distances of the site from three earthquake sources as 153*km*, 253*km* and 87.5*km* respectively; (ii) annual occurrence rate of earthquakes as 4.1, 2.3 and 0.8 respectively; (iii) magnitude of earthquake to vary from 5 to 9 with probability density function (*pdf*) given as $P_M(m) = \beta exp(-\beta(m-m_0))$ where, $\beta = 2.303b$, m_0 is the lower threshold magnitude of earthquake, m is the magnitude of earthquake and b is the relative likelihood of large or small earthquakes and is taken as 0.7. The corresponding 50^{th} percentile risk consistent response spectrum at the bed rock level is shown in Figure (2).

Depth of overlying soil on the bedrock is assumed to be 40*m*. Since base flexibility is important for soft soil condition, the analysis is performed for the soft soil (*Vs*=80*m/sec*). The corresponding free field risk consistent response spectrum is shown in Figure (3), while the free field response spectrum with white noise input at the bed rock level is shown in Figure (4). The soil properties and the values of the spring-dashpot coefficients are shown in Tables (1) and (2). The first five frequencies of the bridge with fixed and flexible bases are compared in Table (3). It is seen from the table that the difference between the first natural frequencies for the two base conditions is about 30%; flexible base provides the less value of the frequency.

The mean value of the ductility factor is taken as 4.0. The ratio between the three components of ground motion R_u (major), R_v(minor) and R_w(vertical) is taken as unity; the angle of incidence (i.e, angle of major earthquake direction with the longitudinal

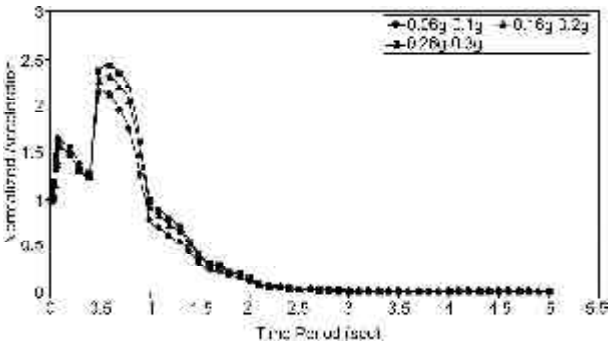

Figure 2. Normalized response spectrum at bedrock.

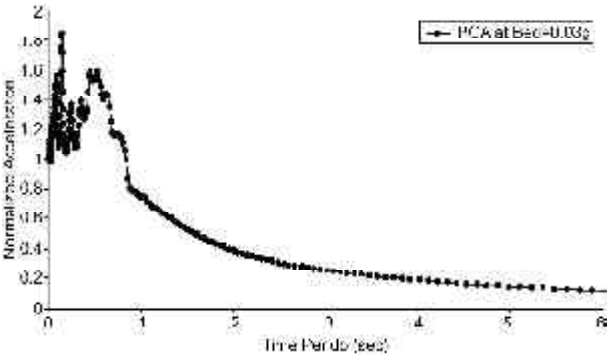

Figure 3. Normalized risk consistent response spectrum at free field (*Vs* = 80m/sec).

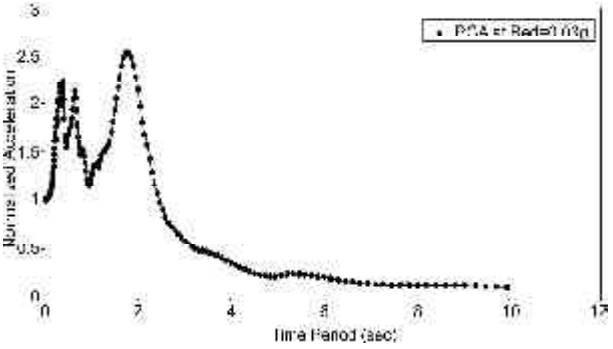

Figure 4. Normalized spectrum at free field for white noise input (Vs = 80m/sec).

Table 1. Equivalent spring and dashpot coefficients for the soil.

Vs = 80m/sec	Horizontal	Vertical	Rotational	Coupled
Stiffness	1.47E+5 KN/m	1.83E+5 KN/m	11.0E+5 KN-m/rad	3.31E+4 KN/rad
Damping	8.82E+4 KN-s/m	1.39E+5 KN-s/m	5.50E+4 KN-s m/rad	2.21E+4 KN-s/rad

Table 2. Equivalent modal damping for the radiation damping of soil.

Modal Damping				
I	II	III	IV	V
5.0 %	10.0 %	17.0 %	25.0 %	34.0 %

Table 3. Natural frequencies for the fixed and flexible base bridges.

Natural Frequencies (rad/sec)					
Mode No.	I	II	III	IV	V
Fixed	2.085	2.989	4.331	4.970	5.957
Flexible	1.496	2.373	4.136	4.849	5.821

axis of the bridge) is taken as zero; shown in Figure (5); the value of correlation coefficient *c* is taken as 0.5, unless mentioned otherwise. The bridge is assumed to fail when a partial failure of bridge deck takes place by forming plastic hinges at point 3 and the corresponding point on the other symmetric half (Figure (1)) where the maximum bending moment occurs. Such partial failure makes the bridge redundant in terms of serviceability. It is assumed that the cross section of the bridge is subjected to 50% of the yield stress because of the superimposed of dead load and gravity load. Therefore, 50% of σ_y value is assumed to be threshold limit for seismic effect.

9.1. Effect of Base Flexibility

Figure (6) shows the comparison between the fragility curves obtained for fixed and flexible base conditions. It is seen from the figures that the probability of failure is significantly less for the flexible base condition. This is the case because the flexible base condition attracts much less lateral load because of two effects namely, increased time period and increased damping. Therefore, soil–structure interaction should not be ignored for obtaining the seismic risk of structures in case of the soft soil condition. Base fixity provides considerably higher estimate of the probability of failure.

9.2. Effect of Degree of Correlation between Support Excitations

Figure (7) shows the comparison between the effects of correlation between support excitations on the probability of failure for the fixed and flexible base conditions. It is seen from the figures that partially correlated ground motion between support excitations provide more probability of failure as compared to the fully correlated ground motion. This is the case

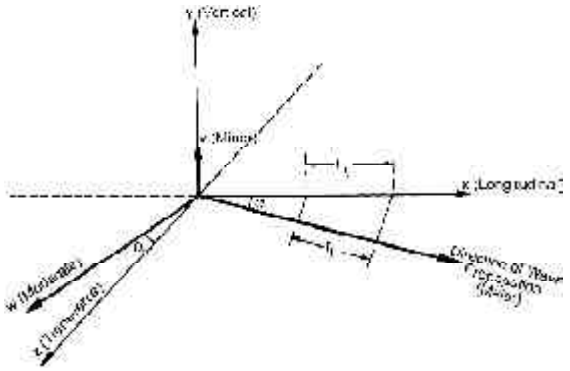

Figure 5. Principal directions of the bridge (x, y, z) and the ground motion (u, v, w).

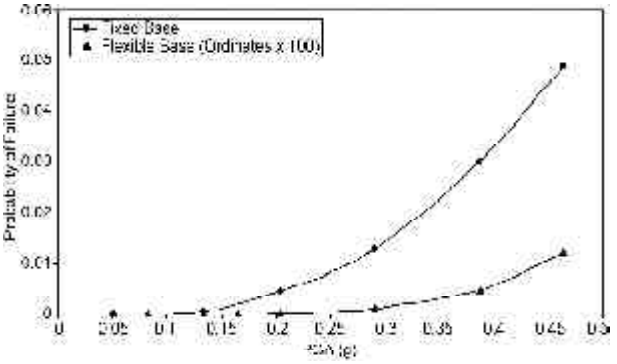

Figure 6. Comparison between fragility curves for flexible and fixed base conditions.

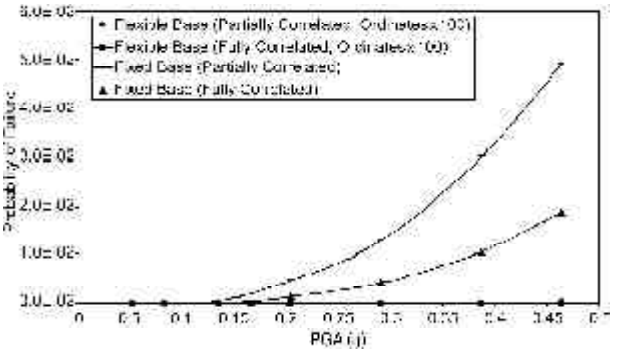

Figure 7. Comparison between fragility curves for different degrees correlation between support excitation.

because the partially correlated ground motion produces more bending moment at the critical nodes for the same level of *PGA*. The difference between probabilities of failure because of the correlation effect increases with the increase in the value of *PGA*. Further, it is seen that the partially correlated ground motion between support excitations with flexible base provides significantly less value of probability of failure as compared to the fixed base; the effect of correlation of ground motion on the probability of failure is more for flexible base condition.

9.3. Effect of Angle of Incidence of Earthquake

Figure (8) shows the effect of angle of incidence of earthquake on the probability of failure. For 0^0 angle of incidence, probability of failure is more as compared to 70^0 angle of incidence. This is caused due to changes in ground motion and its correlation length, used for determining the response of the bridge deck, with the change in the angle of incidence. Further, the effect of the angle of incidence of earthquake on the probability of failure is found to be more for flexible base condition.

9.4. Effect of the Ratio of Components of Ground Motion

Figure (9) shows the effect of the ratio (R_u: R_v: R_w) of the components of ground motion on the probability of failure for the fixed and flexible base conditions. It is seen from the figures that when both R_u and R_v components are maximum of all other values used in different combinations, the probability of failure is maximum. Thus, not only the higher value of the vertical component of ground motion gives higher value of probability of failure but also higher value of P_f is obtained if the longitudinal of ground motion is also more. The reason for this is that longitudinal component of ground motion contributes to the vertical vibration of the deck because of the cable–deck interaction. Further, the effect of the ratio of the components of ground motion on the probability of failure is more for the flexible base condition.

9.5. Effect of Input Response Spectrum

Figure (10) compares between fragility curves obtained with white noise and risk consistent response spectrum inputs at the bed rock level for partially correlated ground motion. It is seen from the figures that the probabilities of failure are significantly changed when the input ground motion at the bedrock

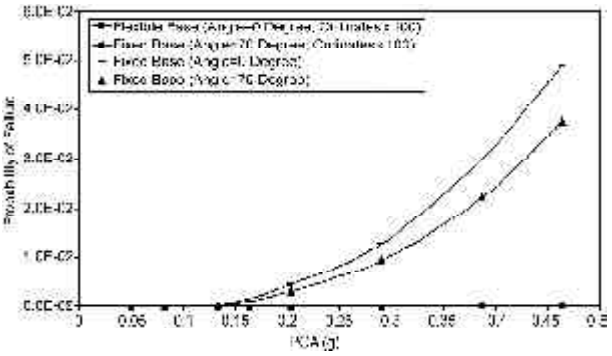

Figure 8. Comparison between fragility curves for different angles of incidence of earthquake.

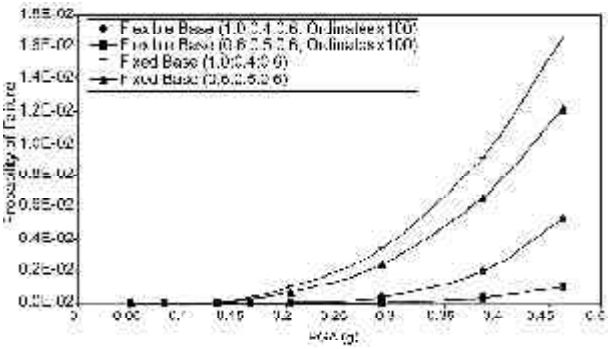

Figure 9. Comparison between fragility curves for different ratios of the components of ground motion.

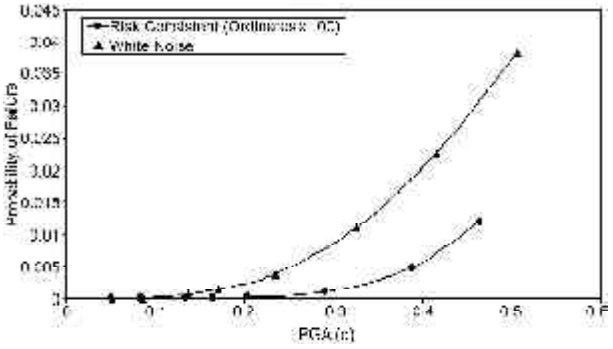

Figure 10. Comparison between fragility curves for different input response spectrums.

is changed to white noise. The white noise input ground motion provides higher values of the probability of failure. This is due to the fact that the local soil amplification is more for the white noise input, see Figure (4).

10. Conclusions

A simplified *PRA* procedure is presented for the seismic risk evaluation of cable stayed bridges with flexible base support arising due to soil-structure interaction (*SSI*). The effect of rotational, lateral and vertical base flexibilities on the response of the

bridge deck is considered by using equivalent modal energy technique. The probability of failure of the bridge is determined with modified frequency and modal damping of the bridge arising due to *SSI*. Uncertainties in the soil properties and approximations in the *SSI* analysis are duly incorporated in the analysis. A three span cable stayed bridge is considered as an illustrative example for the soft soil condition with *Vs*=80*m/sec*. The results of the analysis are compared with those for the fixed base condition under different parametric variations. The results of the study indicate that:

- For the assumed soil layer, the base flexibility due to *SSI* provides about 28% less frequency in the first mode of vibration. The corresponding equivalent modal damping for the soil is about 5%.
- The probability of failure increases with the increase in the ratio of vertical to longitudinal components of ground motion and with the increase of longitudinal component of ground motion itself; the effect is more for flexible base condition.
- Flexible base condition provides significantly less value of probability of failure as compared to the fixed base.
- Fully correlated ground motion between support excitations provides less value of probability of failure as compared to the uncorrelated ground motion; the effect is more for flexible base condition.
- Effect of angle of incidence on the probability of failure is significant and is more for flexible base condition as compared to the fixed base condition.
- When the risk consistent acceleration input spectrum is changed to the response spectrum corresponding to white noise at the bedrock level, the probabilities of failure are considerably increased. Thus, in the absence of a reliable risk consistent input spectrum, white noise input at the bedrock level is a conservative choice for reliability estimates.

References

1. Takemiya, H. and Kai, S. (1983). "Seismic Analysis of a Multi-Span Continuous Elevated Bridge on Deep Pile Foundations", *Proc. JSCE*, **332**, 1-10.

2. Spyrakos, C. (1992). "Seismic Behaviour of Bridge Piers Including Soil-Structure", *Comput. Struct.*, **43**(2), 373-384.

3. Kitazawa, M., Ishizaki, H., Emi, S., and Nishimori, K. (1990). "Characteristics of Earthquake Response and Aseismic Design on the Long Period Cable Stayed Bridge with All Movable Shoes in Longitudinal Direction", *Proc., JSCE,* **422**, 343-352.

4. Kawano, K. and Furukawa, K. (1988). "Random Seismic Response Analysis of Soil Cable Stayed Bridge Interaction", *Proc. 9th WCEE,* **6**, 495-500.

5. Novak, M. (1974), "Effect of Soil on Structural Response to Wind and Earthquake", *Earthquake Engineering and Structural Dynamics,* **3,** 79-86.

6. Veletsos, A.S. and Wei, Y.T. (1971). "Lateral and Rocking Vibrations of Footings", *J. Soil Mech. Found. Div., ASCE,* **97,** 1227-1248.

7. Shinozuka, M., Takeda, M., and Kai, Y. (1989). "Seismic PRA Procedure in Japan and Its Application to a Building Performance Safety Estimation, Part3. Estimation of Building and Equipment Performance Safety", *Proc. ICOSSAR 89, 5th Int. Conference on Structural Safety and Reliability, ASCE*, USA, 637-644.

8. Takemura, M., Ishida, H., Amano, A. and Mizutani, M. (1989). "Seismic PRA Procedure in Japan and Its Application to a Building Performance Safety Estimation, Part1. Fragility Analysis", *Proc. ICOSSAR 89, 5th Int. Conf. Structural Safety and Reliability, ASCE*, USA, 629-636.

9. Der Kiureghian, A. (1981). "A Response Spectrum Method for Random Vibration of MDOF Systems", *Earthquake Engineering and Structural Dynamics,* **9**, 419-435.

10. Takeda, M., Kai, Y, and Mizutani, M. (1989). "Seismic PRA Procedure in Japan and Its Application to a Building Performance Safety Estimation, Part2. Fragility Analysis", *Proc. ICOSSAR 89, 5th Int. Conf. Structural Safety and Reliability, ASCE*, USA, 629-636.

11. Au, F.T.K., Cheng, Y.S., Cheung, Y.K., and Zheng, D.Y. (2001). "On the Determination of Natural Frequencies and Mode Shapes of Cable Stayed Bridge", *Applied Mathematical Modeling,* **2** (25), 1115-1099.

12. Gupta, I.D., Rambabu, V., and Gowda, B.M.R. (1997). "An Integrated PGA Attenuation Relationship", *Bull. Ind. Soc. Earthq. Tech.*, **34**(3), 137-158.